

LINEARLY DECOUPLED ENERGY-STABLE NUMERICAL METHODS FOR MULTI-COMPONENT TWO-PHASE COMPRESSIBLE FLOW*

JISHENG KOU[†], SHUYU SUN[‡], AND XIUHUA WANG[§]

Abstract. In this paper, for the first time we propose two linear, decoupled, energy-stable numerical schemes for multi-component two-phase compressible flow with a realistic equation of state (e.g. Peng-Robinson equation of state). The methods are constructed based on the scalar auxiliary variable (SAV) approaches for Helmholtz free energy and the intermediate velocities that are designed to decouple the tight relationship between velocity and molar densities. The intermediate velocities are also involved in the discrete momentum equation to ensure a consistency relationship with the mass balance equations. Moreover, we propose a component-wise SAV approach for a multi-component fluid, which requires solving a sequence of linear, separate mass balance equations. We prove that the methods have the unconditional energy-dissipation feature. Numerical results are presented to verify the effectiveness of the proposed methods.

Key words. Multi-component two-phase flow; Diffuse interface model; Energy stability; Realistic equation of state.

AMS subject classifications. 65N12; 76T10; 49S05

1. Introduction. It is a very important issue to simulate multi-component two-phase compressible fluid systems with a realistic equation of state (e.g. Peng-Robinson equation of state [28]). It has a wide range of applications in chemical and reservoir engineering [12–17, 27, 30], especially the pore scale modeling of subsurface fluid flow including shale gas reservoir. The classical models of incompressible two-phase flows or compositional flows have been extensively studied and employed [3, 10, 19, 26], the primal state variables of which are often pressure, temperature, and chemical composition. Although the classical models have been widely used, they suffer from a few essential limitations as pointed out in [23, 27]; for example, it is required to construct a pressure equation since there is no intrinsic pressure equation [27].

An alternative modeling framework, which uses the moles, volume, and temperature (the so-called NVT-based framework) as the primal state variables, has been intensively studied recently [12–18, 27, 30]. The NVT-based modeling framework originates from the phase-splitting calculations of multi-component fluids at specified moles, volume and temperature [23]. Very recently, in the NVT-based framework, a general multi-component two-phase compressible flow model is rigorously derived in [21] based on the thermodynamic laws and a realistic equation of state (e.g. Peng-Robinson equation of state). The model developed in [21] has at least three important features that are distinguished from the classical models:

- It has thermodynamically-consistent unified formulations for general average velocities and mass diffusion fluxes;

*This work is supported by National Natural Science Foundation of China (No.11301163), and KAUST research fund to the Computational Transport Phenomena Laboratory.

[†]School of Mathematics and Statistics, Hubei Engineering University, Xiaogan 432000, Hubei, China.

[‡]Corresponding author. Computational Transport Phenomena Laboratory, Division of Physical Science and Engineering, King Abdullah University of Science and Technology, Thuwal 23955-6900, Kingdom of Saudi Arabia. Email: shuyu.sun@kaust.edu.sa.

[§]School of Mathematics and Statistics, Hubei Engineering University, Xiaogan 432000, Hubei, China.

- It uses diffusive interfaces and realistic equations of state, and as a result, it can characterize the fluid compressibility and partial miscibility between different phases;
- It uses a general thermodynamic pressure, which is a function of the molar density and temperature, and consequently, it is never required to construct the pressure equation;

In addition, another formulation of the momentum conservation equation, which is convenient for numerical simulation, has been derived in [21] by the relation between the pressure gradient and chemical potential gradients. In this paper, we consider how to develop and analyze numerical methods for this model problem.

A key challenge in numerical simulation of diffuse interface models is to construct efficient numerical schemes preserving the discrete energy-dissipation law [4, 31]. In constructing energy-stable numerical schemes for multi-component two-phase compressible flow model, there are at least two main difficulties: one is the strong non-linearity of bulk Helmholtz free energy density; the other is the tightly coupling relationship between molar densities and flow velocity through the convection term in the mass balance equations and the stress force arising from chemical potential gradients in the momentum balance equation. An energy-dissipation numerical scheme was developed in [21] based on a convex-concave splitting of Helmholtz free energy density, but it leads to a nonlinear and coupled system of the mass balance equations and momentum balance equation. In this paper, we focus on the linear, decoupled, energy stable numerical schemes.

Recently, for incompressible two-phase flows, a decoupled approach [24] was developed by introducing an intermediate velocity in the phase equation to resolve the coupling relation between the velocity and phase function, and this technique was used to construct linear, decoupled, efficient numerical methods for phase-field models of incompressible two-phase flows [4, 31]. When applying this technique to compressible multi-component two-phase flow model considered in this paper, we encounter two challenging problems: the first is how to construct the intermediate velocities since the stress force in the momentum balance equation is different from phase-field models; the second is how to treat the momentum balance equation using intermediate velocities. The second problem is because at the time-discrete level, the velocity variable in the convection term of the momentum balance equation shall be consistent with the intermediate velocities when we combine the mass balance equation of each component and the momentum balance equation to derive the variation of the kinetic energy. In this work, we will construct two intermediate velocities, both of which can uncouple the relationship between velocity and molar densities; we will also propose a discrete formulation of the momentum balance equation, which involves the intermediate velocities and consequently consistent with the mass balance equations. It is noted that one of the introduced intermediate velocities is for the first time defined by a component-wise way, and thus, it is very efficient for a special multi-component fluid.

There have been at least four approaches in the literature dealing with the bulk Helmholtz free energy density derived from Peng-Robinson equation of state for constructing energy-stable numerical schemes. The first approach is the convex splitting method [7, 8], which has been popularly used in phase-field models [2, 8, 31, 34]. The energy-stable numerical scheme based on the convex splitting method have also been developed and analyzed for the diffuse-interface models with Peng-Robinson equation of state [9, 17, 20, 21, 29, 30]. The second approach is a modified Newton's method with

a relaxation parameter that is dynamically chosen to ensure the energy decay property [15]. The third approach is a fully-implicit unconditionally-stable scheme [16], which uses the difference of Helmholtz free energy density to approximate the chemical potential. The fourth numerical scheme is developed in [22] based on the invariant energy quadratization (IEQ) approach that is a novel, efficient method and has been applied to many phase-field models intensively recently [35–37]. Very recently, a scalar auxiliary variable (SAV) approach [32] is built upon the IEQ approach. It leads to unconditionally stable numerical schemes that only linear equations with constant coefficients need to be solved at each time step. In this paper, we will apply the SAV approach to treat the mass balance equations and construct linear, unconditionally stable numerical schemes. Moreover, we will develop a component-wise SAV approach for a multi-component flow model, which uncouples the relationships between multiple components and allows us to solve each component mass balance equation separately. The schemes for gradient flows of multiple functions in [32] usually require the computation of eigen-matrix and eigenvalues to achieve the decoupled forms, but this computation cost is free for the proposed component-wise SAV approach. So the proposed scheme is efficient and easy-to-implement for the case of multiple components.

We must note that the proposed numerical schemes for multi-component two-phase flows are perfect combinations of the above intermediate velocity approaches and SAV approaches, which lead to a sequence of linearly decoupled equations and are proved to be unconditionally stable.

The rest of this paper is organized as follows. In Section 2, we will give a brief description of the multi-component two-phase flow model. In Section 3, we will propose the numerical schemes and prove the energy stability. In Section 4, numerical tests are carried out to show the effectiveness of the proposed methods. Finally, concluding remarks are provided in Section 5.

2. Mathematical model of multi-component two-phase flow. In this section, we briefly introduce mathematical model of multi-component two-phase flow with Peng-Robinson equation of state, which is very recently proposed in [21].

We consider the motion of a mixture fluid composed of M chemical components at a constant temperature. Let n_i be the molar density of component i , and we denote the molar density vector by $\mathbf{n} = [n_1, n_2, \dots, n_M]^T$.

Mathematical model developed in [21] can employ any realistic equation of state, for instance, the van der Waals equation of state and Peng-Robinson equation of state (PR-EOS) [28]. PR-EOS has been widely applied in oil reservoir and chemical engineering. In this work, we focus on the PR-EOS-based Helmholtz free energy density $f_b(\mathbf{n})$ of a homogeneous bulk fluid, which has a form as

$$f_b(\mathbf{n}) = f_b^{\text{ideal}}(\mathbf{n}) + f_b^{\text{repulsion}}(\mathbf{n}) + f_b^{\text{attraction}}(\mathbf{n}), \quad (2.1)$$

where f_b^{ideal} , $f_b^{\text{repulsion}}$ and $f_b^{\text{attraction}}$ are formulated in Appendix A.

The diffuse interfaces always occurs between multiple phases of a realistic fluid. To characterize this feature, a local density gradient contribution is added to the free energy density of an inhomogeneous fluid, and consequently, the general Helmholtz free energy density (denoted by f) is expressed as

$$f(\mathbf{n}) = f_b(\mathbf{n}) + \frac{1}{2} \sum_{i,j=1}^M c_{ij} \nabla n_i \cdot \nabla n_j, \quad (2.2)$$

where c_{ij} ($1 \leq i, j \leq M$) are the cross influence parameters that are formulated in Appendix B. We assume that the influence parameter matrix $(c_{ij})_{i,j=1}^M$ is symmetric and moreover it is positive definite or positive semi-definite.

The chemical potential of component i is defined as

$$\mu_i(\mathbf{n}) = \frac{\delta f(\mathbf{n})}{\delta n_i} = \mu_i^b(\mathbf{n}) - \sum_{j=1}^M \nabla \cdot (c_{ij} \nabla n_j), \quad \mu_i^b(\mathbf{n}) = \frac{\partial f_b(\mathbf{n})}{\partial n_i}, \quad (2.3)$$

where $\frac{\delta}{\delta n_i}$ denotes the variational derivative. By the thermodynamical relations, the general thermodynamical pressure can be formulated as a function of \mathbf{n} at a constant temperature [21]

$$\begin{aligned} p(\mathbf{n}) &= \sum_{i=1}^M n_i \mu_i(\mathbf{n}) - f(\mathbf{n}) \\ &= p_b - \sum_{i,j=1}^M n_i \nabla \cdot (c_{ij} \nabla n_j) - \frac{1}{2} \sum_{i,j=1}^M c_{ij} \nabla n_i \cdot \nabla n_j, \end{aligned} \quad (2.4)$$

where $p_b(\mathbf{n}) = \sum_{i=1}^M n_i \mu_i^b(\mathbf{n}) - f_b(\mathbf{n})$.

The overall molar density of a mixture is denoted by $n = \sum_{i=1}^M n_i$. Let $M_{w,i}$ denote the molar weight of component i , and then we denote the mass density of component i by $\rho_i = n_i M_{w,i}$ and denote the overall mass density of a mixture by $\rho = \sum_{i=1}^M \rho_i$.

We now describe the governing equations. First, the mass balance equation for component i is

$$\frac{\partial n_i}{\partial t} + \nabla \cdot (\mathbf{u} n_i) + \nabla \cdot \mathbf{J}_i = 0, \quad (2.5)$$

where \mathbf{u} is a specific or average velocity and \mathbf{J}_i is the diffusion flux of component i . In general, we can express the diffusion flux of component i as [5, 18, 21]

$$\mathbf{J}_i = - \sum_{j=1}^M \mathcal{M}_{ij} \nabla \mu_j, \quad i = 1, \dots, M, \quad (2.6)$$

where $\mathcal{M} = (\mathcal{M}_{ij})_{i,j=1}^M$ is the mobility tensor. The mobility matrix \mathcal{M} shall be symmetric and at least positive semidefinite so that Onsager's reciprocal principle [6] and the second law of thermodynamics are satisfied.

Three choices of the mobility \mathcal{M} in (2.6) are provided in [21] as below.

(A1) The first mobility \mathcal{M} is taken as a diagonal positive definite matrix with diagonal elements

$$\mathcal{M}_i = \mathcal{M}_{ii} = \frac{D_i n_i}{RT}, \quad (2.7)$$

where R stands for the universal gas constant and $D_i > 0$ is the diffusion coefficient of component i . The diffusion flux has a form [5, 17] as $\mathbf{J}_i = - \frac{D_i n_i}{RT} \nabla \mu_i$. In this case, \mathbf{u} and \mathbf{J}_i is viewed as mean velocity and general mixture diffusion fluxes at constant temperature and pressure, respectively.

(A2) The second mobility \mathcal{M} is taken as a full matrix

$$\mathcal{M}_{ii} = \sum_{j=1}^M \frac{\mathcal{D}_{ij} n_i n_j}{nRT}, \quad \mathcal{M}_{ij} = -\frac{\mathcal{D}_{ij} n_i n_j}{nRT}, \quad j \neq i, \quad (2.8)$$

where the mole diffusion coefficients \mathcal{D}_{ij} satisfy $\mathcal{D}_{ii} = 0$ and $\mathcal{D}_{ij} = \mathcal{D}_{ji} > 0$ for $i \neq j$. In this case, \mathbf{u} is the molar-average velocity.

(A3) The third mobility \mathcal{M} has the following formulation

$$\mathcal{M}_{ii} = \sum_{j=1}^M \frac{\mathcal{D}_{ij} n_i \rho_j}{M_{w,i} \rho RT}, \quad \mathcal{M}_{ij} = -\frac{\mathcal{D}_{ij} n_i n_j}{\rho RT}, \quad j \neq i, \quad (2.9)$$

where the mass diffusion coefficients \mathcal{D}_{ij} satisfy $\mathcal{D}_{ii} = 0$ and $\mathcal{D}_{ij} = \mathcal{D}_{ji} > 0$ for $i \neq j$. In this case, \mathbf{u} is actually the mass-average velocity.

We now introduce the thermodynamically-consistent momentum balance equation, which is expressed as [21]

$$\begin{aligned} \rho \left(\frac{\partial \mathbf{u}}{\partial t} + \mathbf{u} \cdot \nabla \mathbf{u} \right) + \sum_{i=1}^M M_{w,i} \mathbf{J}_i \cdot \nabla \mathbf{u} = -\nabla p + \nabla (\lambda \nabla \cdot \mathbf{u}) \\ + \nabla \cdot \eta (\nabla \mathbf{u} + \nabla \mathbf{u}^T) - \sum_{i,j=1}^M \nabla \cdot (c_{ij} \nabla n_i \otimes \nabla n_j), \end{aligned} \quad (2.10)$$

where $\lambda = \xi - \frac{2}{3}\eta$, and ξ and η represent the volumetric viscosity and shear viscosity respectively. We assume that $\eta > 0$ and $\xi > \frac{2}{3}\eta$, and thus $\lambda > 0$. If \mathbf{u} is the mass-average velocity, the term $\sum_{i=1}^M M_{w,i} \mathbf{J}_i \cdot \nabla \mathbf{u}$ vanishes, while for the other types of \mathbf{u} , it is crucial to ensure the thermodynamical consistency. It is proved in [21] that the gradients of the pressure and chemical potentials have the following relation

$$\sum_{i=1}^M n_i \nabla \mu_i = \nabla p + \sum_{i,j=1}^M \nabla \cdot (c_{ij} \nabla n_i \otimes \nabla n_j). \quad (2.11)$$

The momentum conservation equation (2.10) is reformulated as

$$\begin{aligned} \rho \left(\frac{\partial \mathbf{u}}{\partial t} + \mathbf{u} \cdot \nabla \mathbf{u} \right) + \sum_{i=1}^M M_{w,i} \mathbf{J}_i \cdot \nabla \mathbf{u} = -\sum_{i=1}^M n_i \nabla \mu_i \\ + \nabla (\lambda \nabla \cdot \mathbf{u}) + \nabla \cdot \eta (\nabla \mathbf{u} + \nabla \mathbf{u}^T), \end{aligned} \quad (2.12)$$

which shows that the fluid motion is driven by the chemical potential gradients.

In this work, we consider numerical schemes for the model formulated by (2.5) and (2.12) coupling with the diffusion flux (2.6) and the chemical potential (2.3). For the boundary conditions, we assume that all boundary terms in (2.5) and (2.12) will vanish when integrating by parts is performed; for example, we can use homogeneous Neumann boundary conditions or periodic boundary conditions.

We assume that $\Omega \subset \mathbb{R}^d (1 \leq d \leq 3)$ is an open, bounded and connected domain with the sufficiently smooth boundary $\partial\Omega$. The Helmholtz free energy and kinetic energy within Ω at a specified time are defined as

$$F = F_b + F_\nabla, \quad F_b = \int_{\Omega} f_b d\mathbf{x}, \quad F_\nabla = \frac{1}{2} \sum_{i,j=1}^M \int_{\Omega} c_{ij} \nabla n_i \cdot \nabla n_j d\mathbf{x},$$

$$E = \frac{1}{2} \int_{\Omega} \rho |\mathbf{u}|^2 d\mathbf{x}. \quad (2.13)$$

It is proved in [21] that the total energy, i.e. the sum of the Helmholtz free energy and kinetic energy, is dissipated with time as

$$\frac{\partial(F + E)}{\partial t} \leq 0. \quad (2.14)$$

In order to use SVG, we define $H(t) = \sqrt{F_b + \sum_{i=1}^M C_{T,i} N_i^t}$, where $N_i^t = \int_{\Omega} n_i d\mathbf{x}$. Here, $C_{T,i} \geq 0$ is the thermodynamical coefficient of component i that may depend on T but independent of molar densities. Then the chemical potentials can be reformulated as

$$\mu_i = \frac{H(t)}{\sqrt{F_b + \sum_{j=1}^M C_{T,j} N_j^t}} \mu_i^b - \sum_{j=1}^M \nabla \cdot (c_{ij} \nabla n_j^{k+1}), \quad (2.15a)$$

$$\frac{\partial H}{\partial t} = \sum_{i=1}^M \int_{\Omega} \frac{\mu_i^b}{2\sqrt{F_b + \sum_{j=1}^M C_{T,j} N_j^t}} \frac{\partial n_i}{\partial t} d\mathbf{x}. \quad (2.15b)$$

The Helmholtz free energy is modified as

$$\mathcal{F} = H^2 + F_{\nabla} - \sum_{i=1}^M C_{T,i} N_i^t.$$

3. Energy-stable numerical methods. In this section, we aim to develop efficient energy-dissipated semi-implicit time marching scheme for simulating the above multi-component flow model. The key difficulties result from the strong nonlinearity of Helmholtz free energy density and fully coupling relations between molar densities and velocity. In this work, our purpose is to uncouple this tightly coupling relations between molar densities and velocity, and from this, we will develop linearly decoupled numerical schemes preserving the feature of energy dissipation.

For the given time interval $\mathcal{I} = (0, T_f]$, where $T_f > 0$, we divide \mathcal{I} into \mathcal{N} subintervals $\mathcal{I}_k = (t_k, t_{k+1}]$, where $t_0 = 0$ and $t_{\mathcal{N}} = T_f$, and we denote $\delta t_k = t_{k+1} - t_k$. For any scalar $v(t)$ or vector $\mathbf{v}(t)$, we denote by v^k or \mathbf{v}^k its approximation at the time t_k . The traditional notations (\cdot, \cdot) and $\|\cdot\|$ are used to represent the inner product and norm of $L^2(\Omega)$, $(L^2(\Omega))^d$ or $(L^2(\Omega))^{d \times d}$ respectively.

3.1. Velocity-density decoupled semi-implicit scheme. We try to develop a decoupled semi-implicit scheme that decouples the tight relationship between molar densities and velocity. This scheme allows us to solve the mass balance equations and momentum equation separately. This scheme can be applied for the model problems with the general diffusion mobility, especially the cases that the mobility is a full tensor.

We denote $\mathbf{n}^k = [n_1^k, n_2^k, \dots, n_M^k]^T$, and define μ_i^{k+1} as

$$\mu_i^{k+1} = \frac{H^{k+1} + H^k}{2\sqrt{F_b(\mathbf{n}^k) + \sum_{j=1}^M C_{T,j} N_j^t}} \mu_i^b(\mathbf{n}^k) - \sum_{j=1}^M \nabla \cdot (c_{ij} \nabla n_j^{k+1}), \quad (3.1a)$$

$$\frac{H^{k+1} - H^k}{\delta t_k} = \sum_{i=1}^M \int_{\Omega} \frac{\mu_i^b(\mathbf{n}^k)}{2\sqrt{F_b(\mathbf{n}^k) + \sum_{j=1}^M C_{T,j} N_j^t}} \frac{n_i^{k+1} - n_i^k}{\delta t_k} d\mathbf{x}. \quad (3.1b)$$

Furthermore, we define an intermediate velocity \mathbf{u}_*^k as

$$\mathbf{u}_*^k = \mathbf{u}^k - \frac{\delta t_k}{\rho^k} \sum_{i=1}^M n_i^k \nabla \mu_i^{k+1}. \quad (3.2)$$

We note that \mathbf{u}_*^k can be viewed as an approximation of \mathbf{u}^{k+1} obtained by neglecting the three parts: the convection term, $\sum_{i=1}^M M_{w,i} \mathbf{J}_i^{k+1} \cdot \nabla \mathbf{u}^{k+1}$, and the viscosity terms, in (3.4).

Using the intermediate velocity \mathbf{u}_*^k , we construct the semi-implicit time scheme for the molar density balance equation (2.5) as

$$\frac{n_i^{k+1} - n_i^k}{\delta t_k} + \nabla \cdot (n_i^k \mathbf{u}_*^k) + \nabla \cdot \mathbf{J}_i^{k+1} = 0, \quad (3.3a)$$

$$\mathbf{J}_i^{k+1} = - \sum_{j=1}^M \mathcal{M}_{ij}^k \nabla \mu_j^{k+1}, \quad (3.3b)$$

where we denote by \mathcal{M}_{ij}^k the mobility coefficients calculated from molar densities \mathbf{n}^k since the mobility coefficients \mathcal{M}_{ij} generally depending on molar densities can be treated explicitly.

We can see that only \mathbf{n}^{k+1} is the unknown variable of the equations (3.3). This means that the use of \mathbf{u}_*^k eliminates the tight coupling relationship between molar densities and velocity. We can solve (3.3) to obtain molar densities \mathbf{n}^{k+1} . Once \mathbf{n}^{k+1} is calculated, we can get μ_i^{k+1} , \mathbf{J}_i^{k+1} and \mathbf{u}_*^k from (3.1), (3.3b) and (3.2) respectively. A semi-implicit scheme for the momentum balance equation (2.12) is formulated as

$$\begin{aligned} \rho^k \frac{\mathbf{u}^{k+1} - \mathbf{u}^k}{\delta t_k} + \rho^k \mathbf{u}_*^k \cdot \nabla \mathbf{u}^{k+1} + \sum_{i=1}^M M_{w,i} \mathbf{J}_i^{k+1} \cdot \nabla \mathbf{u}^{k+1} = - \sum_{i=1}^M n_i^k \nabla \mu_i^{k+1} \\ + \nabla (\lambda^k \nabla \cdot \mathbf{u}^{k+1}) + \nabla \cdot \eta^k (\nabla \mathbf{u}^{k+1} + (\nabla \mathbf{u}^{k+1})^T), \end{aligned} \quad (3.4)$$

which is a linear equation of velocity \mathbf{u}^{k+1} only. In the convection term of (3.4), the use of \mathbf{u}_*^k instead of \mathbf{u}^k is consistent with the mass balance equations as shown in the proof of Theorem 3.1, and moreover, it avoids to use the existing approach in [24, 31] that needs to impose the overall mass equation into the momentum equation for the sake of achieving energy dissipation for phase-field models with the large density ratios. We note that this treatment (i.e., using \mathbf{u}_*^k instead of \mathbf{u}^k in the convection term of the momentum equation) can be directly applied to phase-field models with different densities.

We now prove that the above decoupled scheme satisfies the discrete energy dissipation. To do this, we define the discrete kinetic energy and the modified Helmholtz free energy as

$$E^k = \frac{1}{2} \int_{\Omega} \rho^k |\mathbf{u}^k|^2 d\mathbf{x}, \quad (3.5a)$$

$$\mathcal{F}^k = |H^k|^2 + F_{\nabla}^k - \sum_{i=1}^M C_{T,i} N_i^t, \quad F_{\nabla}^k = \frac{1}{2} \int_{\Omega} \sum_{i,j=1}^M c_{ij} \nabla n_i^k \cdot \nabla n_j^k d\mathbf{x}. \quad (3.5b)$$

THEOREM 3.1. *The modified total (free) energy, i.e., the sum of the modified Helmholtz free energy and kinetic energy, determined by (3.3) and (3.4) associated with (3.1) and (3.2), is dissipated with time steps, i.e.*

$$E^{k+1} + \mathcal{F}^{k+1} \leq E^k + \mathcal{F}^k. \quad (3.6)$$

Proof. We first estimate the difference between $|H^{k+1}|^2$ and $|H^k|^2$ using (3.1b) as

$$\begin{aligned} |H^{k+1}|^2 - |H^k|^2 &= (H^{k+1} + H^k)(H^{k+1} - H^k) \\ &= \sum_{i=1}^M \left(\frac{(H^{k+1} + H^k) \mu_i^b(\mathbf{n}^k)}{2\sqrt{F_b(\mathbf{n}^k) + C_{T,i} N_i^t}}, n_i^{k+1} - n_i^k \right). \end{aligned} \quad (3.7)$$

Since the influence parameter matrix $(c_{ij})_{i,j=1}^M$ is symmetric and it is positive definite or positive semi-definite, we have

$$\begin{aligned} F_{\nabla}^{k+1} - F_{\nabla}^k &= \frac{1}{2} \int_{\Omega} \sum_{i,j=1}^M c_{ij} (\nabla n_i^{k+1} \cdot \nabla n_j^{k+1} - \nabla n_i^k \cdot \nabla n_j^k) d\mathbf{x} \\ &= \frac{1}{2} \int_{\Omega} \sum_{i,j=1}^M c_{ij} (\nabla (n_i^{k+1} - n_i^k) \cdot \nabla n_j^{k+1} + \nabla n_i^k \cdot \nabla (n_j^{k+1} - n_j^k)) d\mathbf{x} \\ &= \sum_{i,j=1}^M (\nabla (n_i^{k+1} - n_i^k), c_{ij} \nabla n_j^{k+1}) - \sum_{i,j=1}^M (c_{ij} \nabla (n_i^{k+1} - n_i^k), \nabla (n_j^{k+1} - n_j^k)) \\ &\leq \sum_{i,j=1}^M (\nabla (n_i^{k+1} - n_i^k), c_{ij} \nabla n_j^{k+1}) \\ &\leq - \sum_{i,j=1}^M (n_i^{k+1} - n_i^k, \nabla \cdot (c_{ij} \nabla n_j^{k+1})). \end{aligned} \quad (3.8)$$

The inequalities (3.7) and (3.8) yield

$$\mathcal{F}^{k+1} - \mathcal{F}^k = |H^{k+1}|^2 - |H^k|^2 + F_{\nabla}^{k+1} - F_{\nabla}^k \leq \sum_{i=1}^M (\mu_i^{k+1}, n_i^{k+1} - n_i^k). \quad (3.9)$$

Substituting (3.3) into (3.9), we derive

$$\begin{aligned} \mathcal{F}^{k+1} - \mathcal{F}^k &\leq -\delta t_k \sum_{i=1}^M (\nabla \cdot (n_i^k \mathbf{u}_*^k) + \nabla \cdot \mathbf{J}_i^{k+1}, \mu_i^{k+1}) \\ &\leq -\delta t_k \sum_{i=1}^M (\nabla \cdot (n_i^k \mathbf{u}_*^k), \mu_i^{k+1}) - \delta t_k \sum_{i,j=1}^M (\mathcal{M}_{ij}^k \nabla \mu_i^{k+1}, \nabla \mu_j^{k+1}). \end{aligned} \quad (3.10)$$

We now turn to consider the difference between E^{k+1} and E^k . We introduce the intermediate kinetic energy as

$$E_*^k = \frac{1}{2} (\rho^k \mathbf{u}_*^k, \mathbf{u}_*^k).$$

The difference between E^{k+1} and E_*^k is estimated as

$$\begin{aligned} E^{k+1} - E_*^k &= \frac{1}{2} (\rho^{k+1}, |\mathbf{u}^{k+1}|^2) - \frac{1}{2} (\rho^k, |\mathbf{u}_*^k|^2) \\ &= \frac{1}{2} (\rho^k, |\mathbf{u}^{k+1}|^2 - |\mathbf{u}_*^k|^2) + \frac{1}{2} (\rho^{k+1} - \rho^k, |\mathbf{u}^{k+1}|^2) \\ &= (\rho^k (\mathbf{u}^{k+1} - \mathbf{u}_*^k), \mathbf{u}^{k+1}) - \frac{1}{2} (\rho^k, |\mathbf{u}^{k+1} - \mathbf{u}_*^k|^2) \\ &\quad + \frac{1}{2} (\rho^{k+1} - \rho^k, |\mathbf{u}^{k+1}|^2) \\ &\leq (\rho^k (\mathbf{u}^{k+1} - \mathbf{u}_*^k), \mathbf{u}^{k+1}) + \frac{1}{2} (\rho^{k+1} - \rho^k, |\mathbf{u}^{k+1}|^2). \end{aligned} \quad (3.11)$$

On the other hand, we have the overall mass balance equation as

$$\frac{\rho^{k+1} - \rho^k}{\delta t_k} + \nabla \cdot (\rho^k \mathbf{u}_*^k) + \sum_{i=1}^M M_{w,i} \nabla \cdot \mathbf{J}_i^{k+1} = 0, \quad (3.12)$$

and taking into account the definition of \mathbf{u}_*^k , we rewrite (3.4) as

$$\begin{aligned} \rho^k \frac{\mathbf{u}^{k+1} - \mathbf{u}_*^k}{\delta t_k} &= -\rho^k \mathbf{u}_*^k \cdot \nabla \mathbf{u}^{k+1} - \sum_{i=1}^M M_{w,i} \mathbf{J}_i^{k+1} \cdot \nabla \mathbf{u}^{k+1} \\ &\quad + \nabla (\lambda^k \nabla \cdot \mathbf{u}^{k+1}) + \nabla \cdot \eta^k (\nabla \mathbf{u}^{k+1} + (\nabla \mathbf{u}^{k+1})^T). \end{aligned} \quad (3.13)$$

Substituting (3.12) and (3.13) into (3.11) yields

$$\begin{aligned} \frac{E^{k+1} - E_*^k}{\delta t_k} &\leq - \left(\rho^k \mathbf{u}_*^k \cdot \nabla \mathbf{u}^{k+1} + \sum_{i=1}^M M_{w,i} \mathbf{J}_i^{k+1} \cdot \nabla \mathbf{u}^{k+1}, \mathbf{u}^{k+1} \right) \\ &\quad + \left(\nabla (\lambda^k \nabla \cdot \mathbf{u}^{k+1}) + \nabla \cdot \eta^k (\nabla \mathbf{u}^{k+1} + (\nabla \mathbf{u}^{k+1})^T), \mathbf{u}^{k+1} \right) \\ &\quad - \frac{1}{2} \left(\nabla \cdot (\rho^k \mathbf{u}_*^k) + \sum_{i=1}^M M_{w,i} \nabla \cdot \mathbf{J}_i^{k+1}, |\mathbf{u}^{k+1}|^2 \right) \\ &\leq - \left\| \sqrt{\lambda^k} \nabla \cdot \mathbf{u}^{k+1} \right\|^2 - \frac{1}{2} \left\| \sqrt{\eta^k} (\nabla \mathbf{u}^{k+1} + (\nabla \mathbf{u}^{k+1})^T) \right\|^2. \end{aligned} \quad (3.14)$$

We apply the definition of \mathbf{u}_*^k to derive

$$\begin{aligned} E_*^k - E^k &= (\rho^k (\mathbf{u}_*^k - \mathbf{u}^k), \mathbf{u}_*^k) - \frac{1}{2} (\rho^k, |\mathbf{u}_*^k - \mathbf{u}^k|^2) \\ &\leq (\rho^k (\mathbf{u}_*^k - \mathbf{u}^k), \mathbf{u}_*^k) \\ &\leq -\delta t_k \sum_{i=1}^M (n_i^k \nabla \mu_i^{k+1}, \mathbf{u}_*^k) \end{aligned}$$

$$\leq \delta t_k \sum_{i=1}^M (\nabla \cdot (n_i^k \mathbf{u}_*^k), \mu_i^{k+1}). \quad (3.15)$$

Combining (3.10), (3.14) and (3.15) yields

$$\begin{aligned} E^{k+1} - E^k + \mathcal{F}^{k+1} - \mathcal{F}^k &\leq -\delta t_k \sum_{i,j=1}^M (\mathcal{M}_{ij}^k \nabla \mu_i^{k+1}, \nabla \mu_j^{k+1}) - \left\| \sqrt{\lambda^k} \nabla \cdot \mathbf{u}^{k+1} \right\|^2 \\ &\quad - \frac{1}{2} \left\| \sqrt{\eta^k} \left(\nabla \mathbf{u}^{k+1} + (\nabla \mathbf{u}^{k+1})^T \right) \right\|^2 \leq 0, \end{aligned} \quad (3.16)$$

which yields the energy dissipation (3.6). \square

3.2. Component-wise, decoupled semi-implicit scheme. For the case that diffusion fluxes have a diagonal mobility tensor, we can design a component-wise, decoupled semi-implicit scheme, which not only decouples the tight relationship between molar densities and velocity, but also solves the mass balance equations by a component-wise way.

We still use $\mathbf{n}^k = [n_1^k, n_2^k, \dots, n_M^k]^T$ to denote the molar density vector at the integer time step k . Furthermore, we introduce the molar density vector at the fractional time step $(k + \frac{i}{M})$ and denote it by $\mathbf{n}^{k+\frac{i}{M}} = [n_1^{k+\frac{i}{M}}, \dots, n_i^{k+\frac{i}{M}}, n_{i+1}^k, \dots, n_M^k]^T$, where $0 \leq i \leq M$, especially $\mathbf{n}^{k+\frac{i}{M}} = \mathbf{n}^k$ for $i = 0$ and $\mathbf{n}^{k+\frac{i}{M}} = \mathbf{n}^{k+1}$ for $i = M$. The discrete chemical potential $\mu_i^{k+\frac{i}{M}}$ ($1 \leq i \leq M$) of component i is defined as

$$\begin{aligned} \mu_i^{k+\frac{i}{M}} &= \frac{H^{k+\frac{i}{M}} + H^{k+\frac{i-1}{M}}}{2\sqrt{F_b(\mathbf{n}^k) + C_{T,i} N_i^t}} \mu_i^b \left(\mathbf{n}^{k+\frac{i-1}{M}} \right) \\ &\quad - \sum_{j=1}^i \nabla \cdot (c_{ij} \nabla n_j^{k+1}) - \sum_{j=i+1}^M \nabla \cdot (c_{ij} \nabla n_j^k), \end{aligned} \quad (3.17a)$$

$$\frac{H^{k+\frac{i}{M}} - H^{k+\frac{i-1}{M}}}{\delta t_k} = \int_{\Omega} \frac{\mu_i^b \left(\mathbf{n}^{k+\frac{i-1}{M}} \right)}{2\sqrt{F_b(\mathbf{n}^k) + C_{T,i} N_i^t}} \frac{n_i^{k+1} - n_i^k}{\delta t_k} d\mathbf{x}. \quad (3.17b)$$

A component-wise intermediate velocity $\mathbf{u}_*^{k+\frac{i}{M}}$ is defined as

$$\mathbf{u}_*^{k+\frac{i}{M}} = \mathbf{u}_*^{k+\frac{i-1}{M}} - \frac{\delta t_k}{\rho^k} n_i^k \nabla \mu_i^{k+\frac{i}{M}}, \quad 1 \leq i \leq M, \quad (3.18)$$

where $\mathbf{u}_*^{k+0} = \mathbf{u}_*^k = \mathbf{u}^k$. Let $\rho_i = M_{w,i} n_i$ be the mass density of component i , and then we introduce a mean intermediate velocity \mathbf{u}_{**}^k as

$$\mathbf{u}_{**}^k = \sum_{i=1}^M \frac{\rho_i^k}{\rho^k} \mathbf{u}_*^{k+\frac{i}{M}}. \quad (3.19)$$

We construct the semi-implicit time scheme for the molar density balance equation (2.5) of component i as

$$\frac{n_i^{k+1} - n_i^k}{\delta t_k} + \nabla \cdot (n_i^k \mathbf{u}_*^{k+\frac{i}{M}}) + \nabla \cdot \mathbf{J}_i^{k+\frac{i}{M}} = 0, \quad (3.20a)$$

$$\mathbf{J}_i^{k+\frac{i}{M}} = -\mathcal{M}_i^k \nabla \mu_i^{k+\frac{i}{M}}, \quad (3.20b)$$

which can be solved separately from $i = 1$ to M . The semi-implicit time numerical for the momentum balance equation is

$$\begin{aligned} \rho^k \frac{\mathbf{u}^{k+1} - \mathbf{u}^k}{\delta t_k} + \rho^k \mathbf{u}_{**}^k \cdot \nabla \mathbf{u}^{k+1} + \sum_{i=1}^M M_{w,i} \mathbf{J}_i^{k+\frac{i}{M}} \cdot \nabla \mathbf{u}^{k+1} = - \sum_{i=1}^M n_i^k \nabla \mu_i^{k+\frac{i}{M}} \\ + \nabla (\lambda^k \nabla \cdot \mathbf{u}^{k+1}) + \nabla \cdot \eta^k \left(\nabla \mathbf{u}^{k+1} + (\nabla \mathbf{u}^{k+1})^T \right). \end{aligned} \quad (3.21)$$

Summing (3.18) from $i = 1$ to M yields

$$\mathbf{u}_*^{k+1} = \mathbf{u}^k - \frac{\delta t_k}{\rho^k} \sum_{i=1}^M n_i^k \nabla \mu_i^{k+\frac{i}{M}}. \quad (3.22)$$

Consequently, the equation (3.21) can be reformulated as

$$\begin{aligned} \rho^k \frac{\mathbf{u}^{k+1} - \mathbf{u}_*^{k+1}}{\delta t_k} + \rho^k \mathbf{u}_{**}^k \cdot \nabla \mathbf{u}^{k+1} + \sum_{i=1}^M M_{w,i} \mathbf{J}_i^{k+\frac{i}{M}} \cdot \nabla \mathbf{u}^{k+1} \\ = \nabla (\lambda^k \nabla \cdot \mathbf{u}^{k+1}) + \nabla \cdot \eta^k \left(\nabla \mathbf{u}^{k+1} + (\nabla \mathbf{u}^{k+1})^T \right). \end{aligned} \quad (3.23)$$

This is a linear equation of velocity \mathbf{u}^{k+1} and easy to be solved. In the convection term of (3.23), we use the mean intermediate velocity \mathbf{u}_{**}^k instead of \mathbf{u}^k or $\mathbf{u}_*^{k+\frac{i}{M}}$ to match the mass balance equations.

It is apparent that the above component-wise approach can be directly applied for the IEQ-based component-wise schemes and for the Cahn-Hilliard-type models studied in [16].

We now prove that the component-wise, decoupled scheme satisfies the discrete energy dissipation.

THEOREM 3.2. *The sum of the modified Helmholtz free energy and kinetic energy determined by (3.20) and (3.23) associated with (3.17), (3.18) and (3.19) is dissipated with time steps, i.e.*

$$E^{k+1} + \mathcal{F}^{k+1} \leq E^k + \mathcal{F}^k, \quad (3.24)$$

where E^k and \mathcal{F}^k are still defined as in (3.5).

Proof. Using (3.17b), we derive the difference between $|H^{k+\frac{i}{M}}|^2$ and $|H^{k+\frac{i-1}{M}}|^2$ ($1 \leq i \leq M$) as

$$\begin{aligned} |H^{k+\frac{i}{M}}|^2 - |H^{k+\frac{i-1}{M}}|^2 &= \left(H^{k+\frac{i}{M}} + H^{k+\frac{i-1}{M}} \right) \left(H^{k+\frac{i}{M}} - H^{k+\frac{i-1}{M}} \right) \\ &= \left(\frac{\left(H^{k+\frac{i}{M}} + H^{k+\frac{i-1}{M}} \right) \mu_i^b \left(\mathbf{n}^{k+\frac{i-1}{M}} \right)}{2\sqrt{F_b(\mathbf{n}^k)} + C_{T,i} N_i^t}, n_i^{k+1} - n_i^k \right). \end{aligned} \quad (3.25)$$

The gradient contribution of Helmholtz free energy at the time step $(k + \frac{i}{M})$ can be expressed as

$$F_{\nabla}^{k+\frac{i}{M}} = \frac{1}{2} \int_{\Omega} \sum_{j,l=1}^i c_{jl} \nabla n_j^{k+1} \cdot \nabla n_l^{k+1} dx + \frac{1}{2} \int_{\Omega} \sum_{j,l=i+1}^M c_{jl} \nabla n_j^k \cdot \nabla n_l^k dx$$

$$+ \sum_{j=1}^i \sum_{l=i+1}^M \int_{\Omega} c_{jl} \nabla n_j^{k+1} \cdot \nabla n_l^k d\mathbf{x}. \quad (3.26)$$

Taking into account $c_{ij} = c_{ji}$ and $c_{ij} > 0$, we derive

$$\begin{aligned} F_{\nabla}^{k+\frac{i}{M}} - F_{\nabla}^{k+\frac{i-1}{M}} &= \frac{1}{2} \int_{\Omega} c_{ii} (\nabla n_i^{k+1} \cdot \nabla n_i^{k+1} - \nabla n_i^k \cdot \nabla n_i^k) d\mathbf{x} \\ &\quad + \int_{\Omega} \sum_{j=1}^{i-1} c_{ij} \nabla (n_i^{k+1} - n_i^k) \cdot \nabla n_j^{k+1} d\mathbf{x} \\ &\quad + \int_{\Omega} \sum_{j=i+1}^M c_{ij} \nabla (n_i^{k+1} - n_i^k) \cdot \nabla n_j^k d\mathbf{x} \\ &\leq \sum_{j=1}^i (\nabla (n_i^{k+1} - n_i^k), c_{ij} \nabla n_j^{k+1}) \\ &\quad + \sum_{j=i+1}^M (\nabla (n_i^{k+1} - n_i^k), c_{ij} \nabla n_j^k) \\ &\leq - \left(n_i^{k+1} - n_i^k, \sum_{j=1}^i \nabla \cdot c_{ij} \nabla n_j^{k+1} + \sum_{j=i+1}^M \nabla \cdot c_{ij} \nabla n_j^k \right). \end{aligned} \quad (3.27)$$

By the definition of $\mu_i^{k+\frac{i}{M}}$ given in (3.17), we obtain from the estimates (3.25) and (3.27) that

$$\begin{aligned} &|H^{k+\frac{i}{M}}|^2 - |H^{k+\frac{i-1}{M}}|^2 + F_{\nabla}^{k+\frac{i}{M}} - F_{\nabla}^{k+\frac{i-1}{M}} \\ &\leq \left(\mu_i^{k+\frac{i}{M}}, n_i^{k+1} - n_i^k \right) \\ &\leq -\delta t_k \left(\mu_i^{k+\frac{i}{M}}, \nabla \cdot (n_i^k \mathbf{u}_{\star}^{k+\frac{i}{M}}) - \nabla \cdot \mathcal{M}_i^k \nabla \mu_i^{k+\frac{i}{M}} \right) \\ &\leq \delta t_k \left(\mathbf{u}_{\star}^{k+\frac{i}{M}}, n_i^k \nabla \mu_i^{k+\frac{i}{M}} \right) - \delta t_k \left\| \sqrt{\mathcal{M}_i^k} \nabla \mu_i^{k+\frac{i}{M}} \right\|^2, \end{aligned} \quad (3.28)$$

where the second equality is obtained by using (3.20). Summing up (3.28) from $i = 1$ to M yields

$$\begin{aligned} \mathcal{F}^{k+1} - \mathcal{F}^k &= |H^{k+1}|^2 - |H^k|^2 + F_{\nabla}^{k+1} - F_{\nabla}^k \\ &= \sum_{i=1}^M \left(|H^{k+\frac{i}{M}}|^2 - |H^{k+\frac{i-1}{M}}|^2 + F_{\nabla}^{k+\frac{i}{M}} - F_{\nabla}^{k+\frac{i-1}{M}} \right) \\ &\leq \delta t_k \sum_{i=1}^M \left(\mathbf{u}_{\star}^{k+\frac{i}{M}}, n_i^k \nabla \mu_i^{k+\frac{i}{M}} \right) - \delta t_k \sum_{i=1}^M \left\| \sqrt{\mathcal{M}_i^k} \nabla \mu_i^{k+\frac{i}{M}} \right\|^2. \end{aligned} \quad (3.29)$$

We define the intermediate kinetic energy as

$$E_{\star}^{k+\frac{i}{M}} = \frac{1}{2} \left(\rho^k \mathbf{u}_{\star}^{k+\frac{i}{M}}, \mathbf{u}_{\star}^{k+\frac{i}{M}} \right).$$

Using the definition (3.18) of intermediate velocities, we derive

$$\begin{aligned}
E_\star^{k+\frac{i}{M}} - E_\star^{k+\frac{i-1}{M}} &= \frac{1}{2} \left(\rho^k \mathbf{u}_\star^{k+\frac{i}{M}}, \mathbf{u}_\star^{k+\frac{i}{M}} \right) - \frac{1}{2} \left(\rho^k \mathbf{u}_\star^{k+\frac{i-1}{M}}, \mathbf{u}_\star^{k+\frac{i-1}{M}} \right) \\
&= \left(\rho^k \left(\mathbf{u}_\star^{k+\frac{i}{M}} - \mathbf{u}_\star^{k+\frac{i-1}{M}} \right), \mathbf{u}_\star^{k+\frac{i}{M}} \right) - \frac{1}{2} \left(\rho^k, \left| \mathbf{u}_\star^{k+\frac{i}{M}} - \mathbf{u}_\star^{k+\frac{i-1}{M}} \right|^2 \right) \\
&\leq \left(\rho^k \left(\mathbf{u}_\star^{k+\frac{i}{M}} - \mathbf{u}_\star^{k+\frac{i-1}{M}} \right), \mathbf{u}_\star^{k+\frac{i}{M}} \right) \\
&= -\delta t_k \left(n_i^k \nabla \mu_i^{k+\frac{i}{M}}, \mathbf{u}_\star^{k+\frac{i}{M}} \right). \tag{3.30}
\end{aligned}$$

The sum of (3.20) multiplied by $M_{w,i}$ leads to the overall mass balance equation

$$\frac{\rho^{k+1} - \rho^k}{\delta t_k} = -\nabla \cdot (\rho^k \mathbf{u}_{\star\star}^k) - \sum_{i=1}^M M_{w,i} \nabla \cdot \mathbf{J}_i^{k+\frac{i}{M}}, \tag{3.31}$$

where (3.19) is also used to get the first term on the right-hand side. We estimate the difference between E^{k+1} and E_\star^k as

$$\begin{aligned}
\frac{E^{k+1} - E_\star^{k+1}}{\delta t_k} &= \frac{1}{2\delta t_k} (\rho^{k+1}, |\mathbf{u}^{k+1}|^2) - \frac{1}{2\delta t_k} (\rho^k, |\mathbf{u}_\star^{k+1}|^2) \\
&\leq \left(\rho^k \frac{\mathbf{u}^{k+1} - \mathbf{u}_\star^{k+1}}{\delta t_k}, \mathbf{u}^{k+1} \right) + \frac{1}{2} \left(\frac{\rho^{k+1} - \rho^k}{\delta t_k}, |\mathbf{u}^{k+1}|^2 \right) \\
&\leq - \left(\rho^k \mathbf{u}_{\star\star}^k \cdot \nabla \mathbf{u}^{k+1} + \sum_{i=1}^M M_{w,i} \mathbf{J}_i^{k+\frac{i}{M}} \cdot \nabla \mathbf{u}^{k+1}, \mathbf{u}^{k+1} \right) \\
&\quad + \left(\nabla (\lambda^k \nabla \cdot \mathbf{u}^{k+1}) + \nabla \cdot \eta^k \left(\nabla \mathbf{u}^{k+1} + (\nabla \mathbf{u}^{k+1})^T \right), \mathbf{u}^{k+1} \right) \\
&\quad - \frac{1}{2} \left(\nabla \cdot (\rho^k \mathbf{u}_{\star\star}^k) + \sum_{i=1}^M M_{w,i} \nabla \cdot \mathbf{J}_i^{k+\frac{i}{M}}, |\mathbf{u}^{k+1}|^2 \right) \\
&\leq - \left\| \sqrt{\lambda^k} \nabla \cdot \mathbf{u}^{k+1} \right\|^2 - \frac{1}{2} \left\| \sqrt{\eta^k} \left(\nabla \mathbf{u}^{k+1} + (\nabla \mathbf{u}^{k+1})^T \right) \right\|^2, \tag{3.32}
\end{aligned}$$

where the third equality is obtained by using (3.23) and (3.31). Combining (3.30) and (3.32) yields

$$\begin{aligned}
E^{k+1} - E^k &= E^{k+1} - E_\star^{k+1} + \sum_{i=1}^M \left(E_\star^{k+\frac{i}{M}} - E_\star^{k+\frac{i-1}{M}} \right) \\
&\leq -\delta t_k \left\| \sqrt{\lambda^k} \nabla \cdot \mathbf{u}^{k+1} \right\|^2 - \frac{1}{2} \delta t_k \left\| \sqrt{\eta^k} \left(\nabla \mathbf{u}^{k+1} + (\nabla \mathbf{u}^{k+1})^T \right) \right\|^2 \\
&\quad - \delta t_k \sum_{i=1}^M \left(n_i^k \nabla \mu_i^{k+\frac{i}{M}}, \mathbf{u}_\star^{k+\frac{i}{M}} \right). \tag{3.33}
\end{aligned}$$

Finally, it is derived from (3.29) and (3.33) that

$$\begin{aligned}
E^{k+1} - E^k + \mathcal{F}^{k+1} - \mathcal{F}^k &\leq -\delta t_k \left\| \sqrt{\mathcal{M}_i^k} \nabla \mu_i^{k+\frac{i}{M}} \right\|^2 - \delta t_k \left\| \sqrt{\lambda^k} \nabla \cdot \mathbf{u}^{k+1} \right\|^2 \\
&\quad - \frac{1}{2} \delta t_k \left\| \sqrt{\eta^k} \left(\nabla \mathbf{u}^{k+1} + (\nabla \mathbf{u}^{k+1})^T \right) \right\|^2, \tag{3.34}
\end{aligned}$$

which yields the energy dissipation (3.24). \square

4. Numerical tests. In this section, we apply the proposed methods to simulate multi-component two-phase flow problems. A binary mixture and a ternary mixture are considered under different conditions. We consider a square domain with the length 20 nm, and we use a uniform rectangular mesh with 40×40 elements. For spatial discretization, the cell-centered finite difference method and the upwind scheme are employed to discretize the mass balance equation, and the finite volume method on the staggered mesh [33] is applied for the momentum balance equation. We note that the above spatial discretization methods have equivalent relationships with special mixed finite element methods under specified quadrature rules [1, 11].

4.1. Binary mixture. In this example, we consider a binary mixture composed of methane (C_1) and pentane (C_5) at a constant temperature 310 K. At the initial time, a square shape droplet is located in the center of the domain. The initial gas molar densities of C_1 and C_5 are 7.4302 kmol/m^3 and 0.6736 kmol/m^3 respectively, while the initial liquid molar densities of C_1 and C_5 are 6.8663 kmol/m^3 and 4.7915 kmol/m^3 respectively. The initial molar density distributions for C_1 and C_5 are illustrated in Figure 4.2(a) and (d) respectively. We use the mole-average velocity and take the diffusion mobility formulation given by (2.8) with $\mathcal{D}_{12} = \mathcal{D}_{21} = 10^{-8} \text{ m}^2/\text{s}$. The volumetric viscosity and the shear viscosity are taken as $\xi = \eta = 10^{-4} \text{ Pa}\cdot\text{s}$. The time step size is taken as 10^{-12} s , and 200 time steps are simulated.

The velocity-density decoupled method proposed in Sub-section 3.1 is applied to simulate the dynamical evolution of the square-shaped droplet. In Figure 4.1, we show the evolution profiles of the modified total energy (i.e., the sum of the modified Helmholtz free energy and kinetic energy) with time steps; we also depict the original total energy (i.e., the sum of the original Helmholtz free energy and kinetic energy) for the sake of comparison. It is observed from Figure 4.1(a) that although the modified total (free) energy is slightly less than the original energy, both total (free) energies are strictly dissipated with time steps, and moreover, Figure 4.1(b), which is a zoom-in plot of Figure 4.1(a) in the later time steps, demonstrates that both total (free) energies remain to decrease. As a result, the proposed method can preserve the energy-dissipation feature.

Figure 4.2 depicts the evolution process of each component molar density, and it is clearly observed that the droplet is gradually reshaped to a circle from its initial square shape due to chemical potential gradients. In Figures 4.3, we show the fluid motion driven by chemical potential gradients, including the velocity field and magnitudes of both velocity components.

4.2. Ternary mixture. In this example, we consider a ternary mixture composed of methane (C_1) pentane (C_5) and decane (C_{10}) at a constant temperature 323 K. The initial gas molar densities of C_1 , C_5 and C_{10} are 10.516 kmol/m^3 , 0.77 kmol/m^3 and 0.184 kmol/m^3 respectively, while the initial liquid molar densities of C_1 , C_5 and C_{10} are 7.8412 kmol/m^3 , 1.9925 kmol/m^3 and 1.433 kmol/m^3 respectively. At the initial time, there are two square-shaped droplets in the domain, as shown in the first figures of Figures 4.5, 4.6 and 4.7 respectively. The diffusion fluxes are formulated by (2.7) with the diffusion coefficients $D_i = 3 \times 10^{-8} \text{ m}^2/\text{s}$ ($1 \leq i \leq 3$). The volumetric viscosity and the shear viscosity are set as $\xi = \eta = 10^{-4} \text{ Pa}\cdot\text{s}$. We take the time step size equal to 10^{-12} s , and we simulate the evolution process for 1000 time steps.

We employ the component-wise, decoupled numerical scheme proposed in Sub-section 3.2. We depict the original and modified total energies and their zoom-in plots in Figure 4.4. We still see that both of total energies are dissipated with time steps.

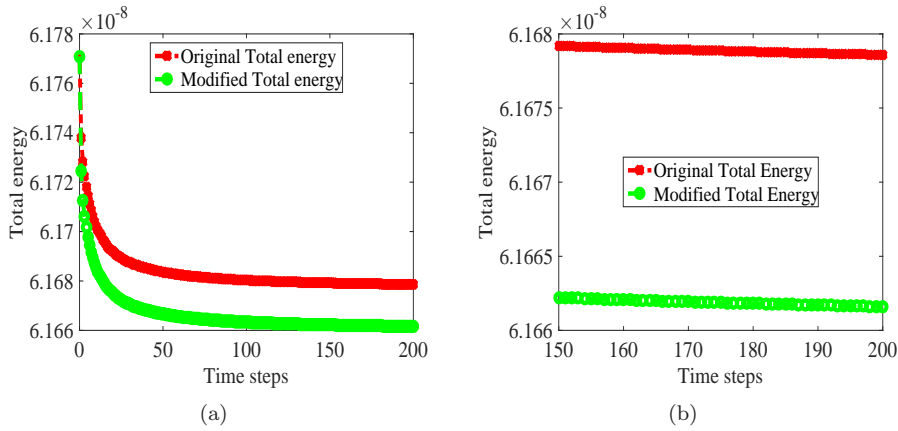


Fig. 4.1: Binary mixture: total energy dissipation with time steps.

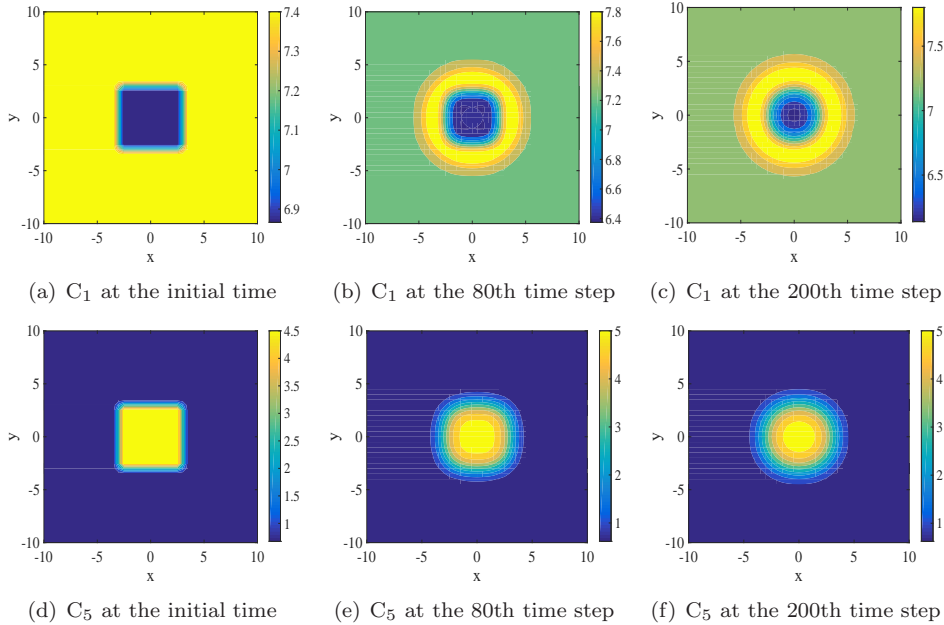


Fig. 4.2: Binary mixture: molar densities of C_1 and C_5 at different time steps.

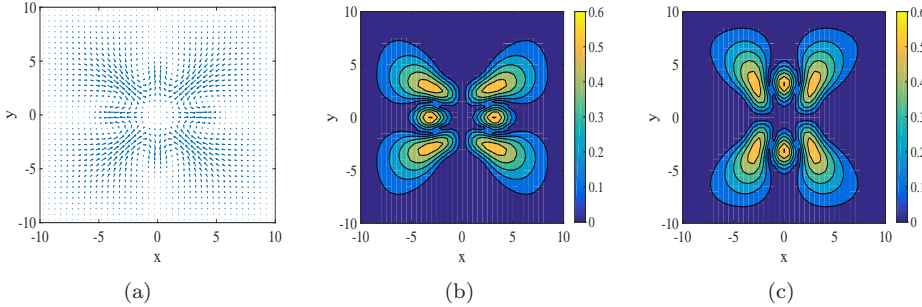


Fig. 4.3: Binary mixture: (a) flow quiver, (b) magnitude contour of x -direction velocity component, and (c) magnitude contour of y -direction velocity component at the 80th time step.

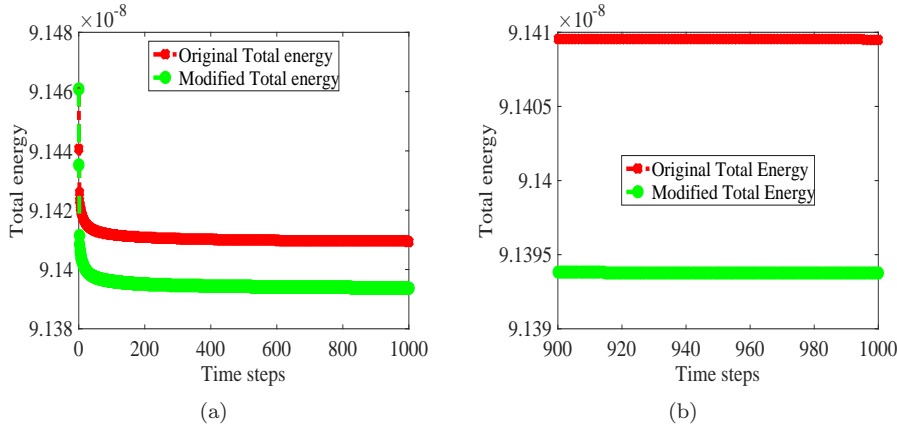


Fig. 4.4: Ternary mixture: energy dissipation with time steps.

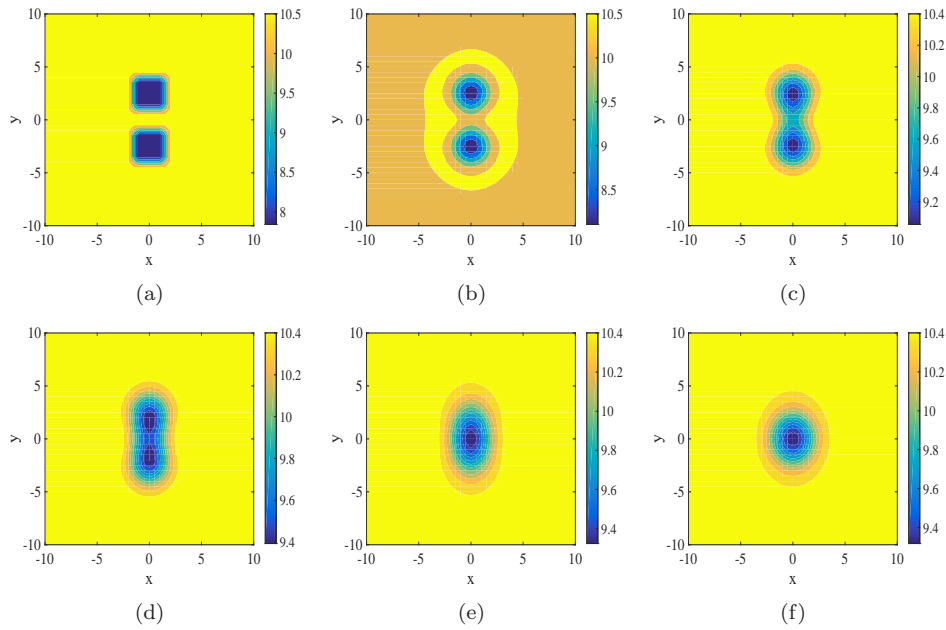


Fig. 4.5: Ternary mixture: CH₄ molar densities at the the initial(a), 30th(b), 100th(c), 200th(d), 500th(e) and 1000th(f) time step respectively.

We also note that in practical computations, the component-wise method is really effective for the mixtures composed of more components since it just needs to solve one more mass-balance equation as a new component is added.

Figures 4.5, 4.6 and 4.7 illustrate the molar density configurations of ternary components. In Figure 4.8, we depict the fluid motion, including the velocity fields and magnitudes of velocity components, at different time steps. The simulation results show that due to chemical potential gradients, two droplets are first emerging with each other, and at the later time, the merged droplets are gradually reshaped into a circle.

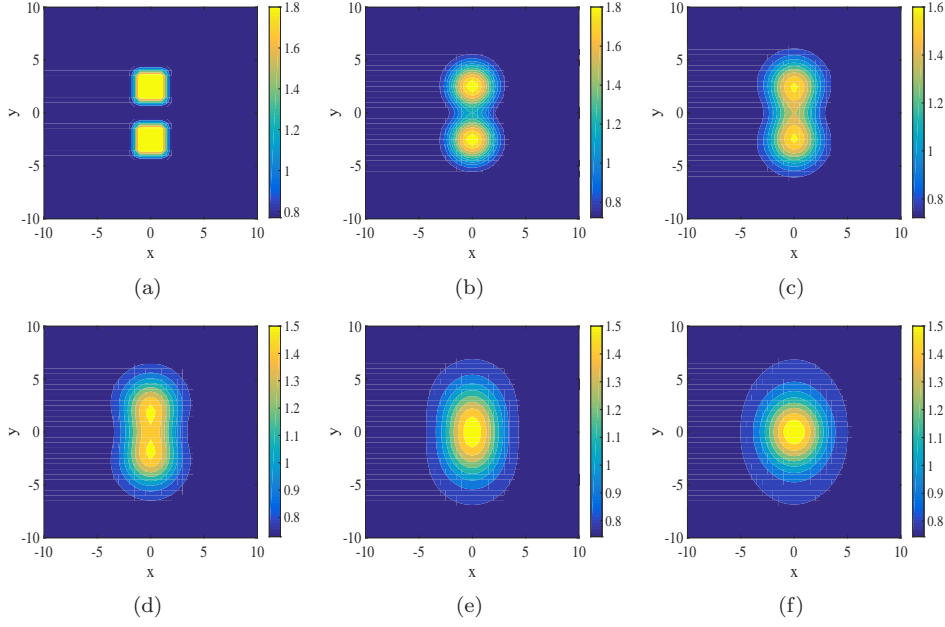


Fig. 4.6: Ternary mixture: C_5 molar densities at the initial(a), 30th(b), 100th(c), 200th(d), 500th(e) and 1000th(f) time step respectively.

5. Conclusions. Two decoupled energy-stable numerical schemes are developed for multi-component two-phase compressible flows with a realistic equation of state (e.g. Peng-Robinson equation of state). In these methods, the scalar auxiliary variable (SAV) approach is applied to deal with the bulk Helmholtz free energy, and moreover, we propose a component-wise SAV approach, which is extremely efficient and easy-to-implement for multi-component flows. In order to uncouple the tight relationship between velocity and molar densities, we introduce two intermediate velocities, one of which has a component-wise form matching the component-wise SAV approach. The intermediate velocities are involved in the discrete formulation of the momentum balance equation, which builds a consistency relationship with the mass balance equations. The proposed numerical schemes only need to solve a sequence of linear equations at each time step. The discrete unconditional energy dissipation laws of the proposed methods are proved rigorously. Numerical results validate the effectiveness of the proposed methods.

Appendix A. Helmholtz free energy density. Let R be the universal gas constant and let T be the specified temperature. The three contributions of Helmholtz free energy density $f_b(\mathbf{n})$ based on Peng-Robinson equation of state are formulated as

$$f_b^{\text{ideal}}(\mathbf{n}) = RT \sum_{i=1}^M n_i (\ln n_i - 1), \quad (\text{A.1})$$

$$f_b^{\text{repulsion}}(\mathbf{n}) = -nRT \ln(1 - bn), \quad (\text{A.2})$$

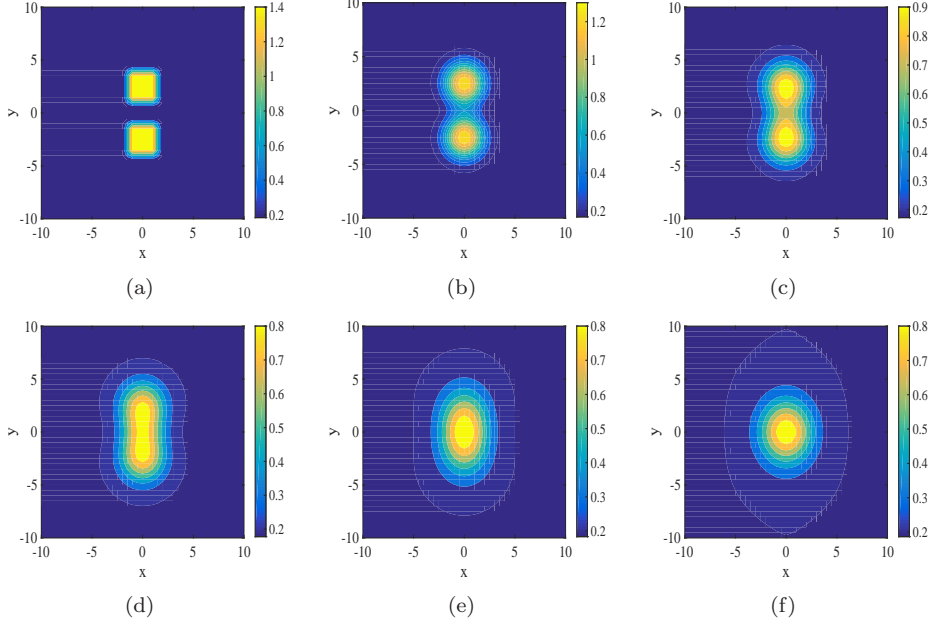


Fig. 4.7: Ternary mixture: C_{10} molar densities at the initial(a), 30th(b), 100th(c), 200th(d), 500th(e) and 1000th(f) time step respectively.

$$f_b^{\text{attraction}}(\mathbf{n}) = \frac{a(T)n}{2\sqrt{2}b} \ln \left(\frac{1 + (1 - \sqrt{2})bn}{1 + (1 + \sqrt{2})bn} \right), \quad (\text{A.3})$$

where $n = \sum_{i=1}^M n_i$ is the overall molar density. Here, a and b are the energy parameter and the covolume respectively, which depend on the mixture composition and temperature. Let us denote by T_{c_i} and P_{c_i} the critical temperature and critical pressure of component i respectively. For the i th component, we let the reduced temperature be $T_{r_i} = T/T_{c_i}$. The parameters a_i and b_i are calculated as

$$a_i = 0.45724 \frac{R^2 T_{c_i}^2}{P_{c_i}} \left[1 + m_i (1 - \sqrt{T_{r_i}}) \right]^2, \quad b_i = 0.07780 \frac{R T_{c_i}}{P_{c_i}}. \quad (\text{A.4})$$

We denote by ω_i the acentric factor of component i . The coefficients m_i are calculated by the following relations

$$m_i = 0.37464 + 1.54226\omega_i - 0.26992\omega_i^2, \quad \omega_i \leq 0.49,$$

$$m_i = 0.379642 + 1.485030\omega_i - 0.164423\omega_i^2 + 0.016666\omega_i^3, \quad \omega_i > 0.49.$$

We denote by $y_i = n_i/n$ the mole fraction of component i and let k_{ij} be the binary interaction coefficients for the energy parameters. Then we calculate $a(T)$ and b as

$$a = \sum_{i=1}^M \sum_{j=1}^M y_i y_j (a_i a_j)^{1/2} (1 - k_{ij}), \quad b = \sum_{i=1}^M y_i b_i.$$

We list some physical parameters of three substances in Table A.1.

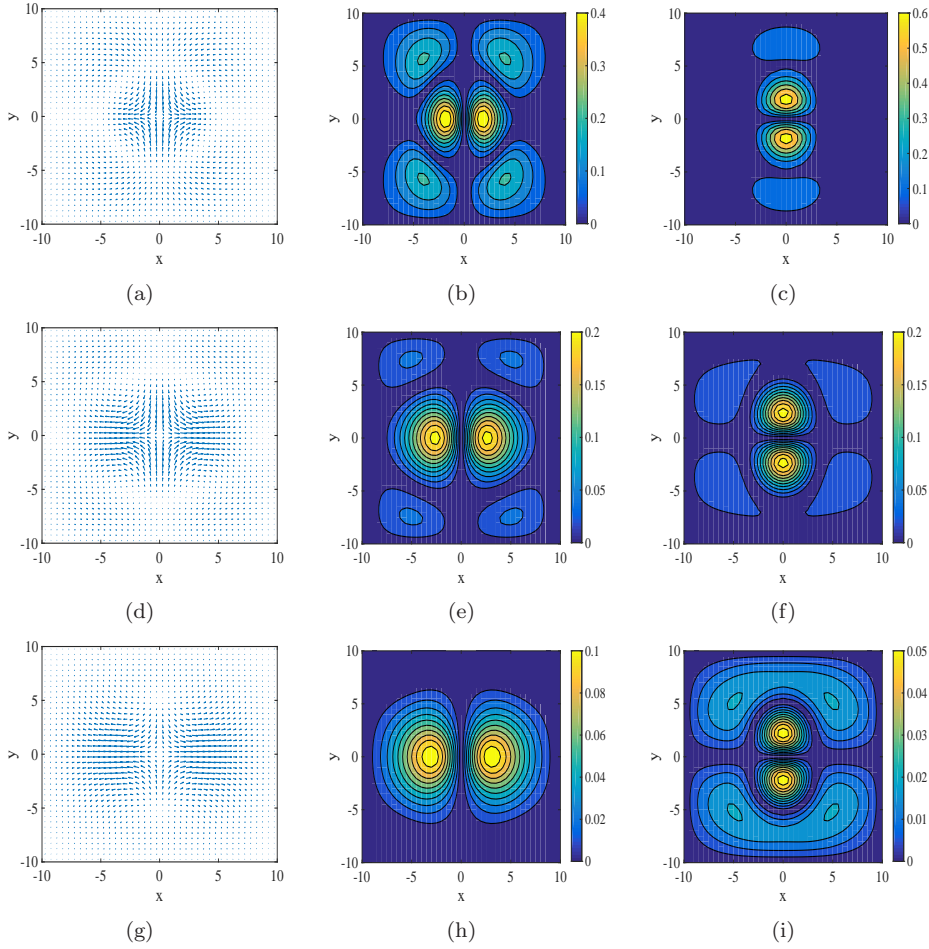


Fig. 4.8: Ternary mixture: flow quivers (left column), magnitude contours of x -direction velocity component (center column), and magnitude contours of y -direction velocity component (right column) at the 100th(top row), 500th(center row), and 1000th(bottom row) time step respectively.

Table A.1: Physical parameters

Substance	P_c (bar)	T_c (K)	Acentric factor	M_w (g/mole)
methane	45.99	190.56	0.011	16.04
pentane	33.70	469.7	0.251	72.15
decane	21.1	617.7	0.489	142.28

Appendix B. Influence parameters. The influence parameters are generally assumed to rely on the temperature but independent of molar densities. We now provide the formulations of the influence parameters. First, we formulate the influence parameter c_i of component i as [25]

$$c_i = a_i b_i^{2/3} [\gamma_i (1 - T_{r_i}) + \phi_i],$$

where a_i and b_i are given in (A.4), and γ_i and ϕ_i are the coefficients correlated merely

with the acentric factor ω_i of component i by the following relations

$$\gamma_i = -\frac{10^{-16}}{1.2326 + 1.3757\omega_i}, \quad \phi_i = \frac{10^{-16}}{0.9051 + 1.5410\omega_i}.$$

The cross influence parameter between binary components is generally calculated as a modified geometric mean of the pure component influence parameters c_i and c_j

$$c_{ij} = (1 - \beta_{ij})\sqrt{c_i c_j},$$

where β_{ij} are the binary interaction coefficients satisfying the symmetry $c_{ij} = c_{ji}$ and $\beta_{ii} = 0$.

REFERENCES

- [1] T. Arbogast, M.F. Wheeler, and I. Yotov. Mixed finite elements for elliptic problems with tensor coefficients as cell-centered finite differences. *SIAM Journal on Numerical Analysis*, 34(2): 828–852, 1997.
- [2] A. Baskaran, J. Lowengrub, C. Wang, S. Wise. Convergence analysis of a second order convex splitting scheme for the modified phase field crystal equation. *SIAM Journal on Numerical Analysis*, 51(5): 2851–2873, 2013.
- [3] Z. Chen, G. Huan, Y. Ma, Computational methods for multiphase flows in porous media. SIAM Comp. Sci. Eng., Philadelphia, 2006.
- [4] Y. Chen, J. Shen. Efficient, adaptive energy stable schemes for the incompressible Cahn-Hilliard Navier-Stokes phase-field models. *Journal of Computational Physics*, 308: 40-56, 2016.
- [5] D. A. Cogswell. *A phase-field study of ternary multiphase microstructures*. PhD thesis, MIT, USA, 2010.
- [6] S. R. De Groot, and P. Mazur. *Non-Equilibrium Thermodynamics*. Dover Publications, New York, 2011.
- [7] C. M. Elliott and A. M. Stuart, The global dynamics of discrete semilinear parabolic equations, *SIAM Journal on Numerical Analysis*, 30: 1622–1663, 1993.
- [8] D. J. Eyre. Unconditionally gradient stable time marching the Cahn-Hilliard equation. *Computational and mathematical models of microstructural evolution (San Francisco, CA, 1998)*, Mater. Res. Soc. Sympos. Proc., 529: 39–46. MRS, Warrendale, PA, 1998.
- [9] X. Fan, J. Kou, Z. Qiao, S. Sun. A Componentwise Convex Splitting Scheme for Diffuse Interface Models with Van der Waals and Peng–Robinson Equations of State. *SIAM Journal on Scientific Computing*, 39(1): B1–B28, 2017.
- [10] A. Firoozabadi. *Thermodynamics of hydrocarbon reservoirs*. McGraw-Hill New York, 1999.
- [11] V. Girault, H. Lopez. Finite-element error estimates for the MAC scheme. *IMA Journal of Numerical Analysis*, 16(3): 347-379, 1996.
- [12] T. Jindrová and J. Mikyška. Fast and robust algorithm for calculation of two-phase equilibria at given volume, temperature, and moles. *Fluid Phase Equilibria*, 353:101–114, 2013.
- [13] T. Jindrová and J. Mikyška. General algorithm for multiphase equilibria calculation at given volume, temperature, and moles. *Fluid Phase Equilibria*, 393:7–25, 2015.
- [14] J. Kou, S. Sun, and X. Wang. Efficient numerical methods for simulating surface tension of multi-component mixtures with the gradient theory of fluid interfaces. *Computer Methods in Applied Mechanics and Engineering*, 292: 92–106, 2015.
- [15] J. Kou and S. Sun. Numerical methods for a multi-component two-phase interface model with geometric mean influence parameters. *SIAM Journal on Scientific Computing*, 37(4): B543–B569, 2015.
- [16] J. Kou and S. Sun. Unconditionally stable methods for simulating multi-component two-phase interface models with Peng-Robinson equation of state and various boundary conditions. *Journal of Computational and Applied Mathematics*, 291(1): 158–182, 2016.
- [17] J. Kou and S. Sun. A stable algorithm for calculating phase equilibria with capillarity at specified moles, volume and temperature using a dynamic model. *Fluid Phase Equilibria*, 456: 7–24, 2018.

- [18] J. Kou and S. Sun. Multi-scale diffuse interface modeling of multi-component two-phase flow with partial miscibility. *Journal of Computational Physics*, 318: 349–372, 2016.
- [19] J. Kou and S. Sun. Convergence of discontinuous Galerkin methods for incompressible two-phase flow in heterogeneous media. *SIAM Journal on Numerical Analysis*, 51: 3280–3306, 2013.
- [20] J. Kou, S. Sun. Efficient energy-stable dynamic modeling of compositional grading. *International Journal of Numerical Analysis and Modeling*, 14(2):218–242, 2017.
- [21] J. Kou and S. Sun. Thermodynamically consistent modeling and simulation of multi-component two-phase flow with partial miscibility. *Computer Methods in Applied Mechanics and Engineering*, 2017.
- [22] H. Li, L. Ju, C. Zhang, Q. Peng. Unconditionally energy stable linear schemes for the diffuse interface model with Peng-Robinson equation of state. *Journal of Scientific Computing*, DOI 10.1007/s10915-017-0576-7, 2017.
- [23] J. Mikyška and A. Firoozabadi. A new thermodynamic function for phase-splitting at constant temperature, moles, and volume. *AIChE Journal*, 57(7):1897–1904, 2011.
- [24] S. Minjeaud. An Unconditionally Stable Uncoupled Scheme for a Triphasic Cahn-Hilliard/Navier-Stokes Model. *Numerical Methods for Partial Differential Equations*, 29(2): 584–618, 2013.
- [25] C. Miqueu, B. Mendiboure, C. Graciaa and J. Lachaise. Modelling of the surface tension of binary and ternary mixtures with the gradient theory of fluid interfaces. *Fluid Phase Equilibria*, 218:189–203, 2004.
- [26] J. Moortgat and A. Firoozabadi. Higher-order compositional modeling of three-phase flow in 3D fractured porous media based on cross-flow equilibrium. *Journal of Computational Physics*, 250: 425–445, 2013.
- [27] O. Polívka and J. Mikyška. Compositional modeling in porous media using constant volume flash and flux computation without the need for phase identification. *Journal of Computational Physics*, 272:149–169, 2014.
- [28] D. Peng and D.B. Robinson. A new two-constant equation of state. *Industrial and Engineering Chemistry Fundamentals*, 15(1):59–64, 1976.
- [29] Q. Peng. A convex-splitting scheme for a diffuse interface model with Peng-Robinson equation of state. *Advances in Applied Mathematics and Mechanics*, 9(5): 1162–1188, 2017.
- [30] Z. Qiao and S. Sun. Two-phase fluid simulation using a diffuse interface model with Peng-Robinson equation of state. *SIAM Journal on Scientific Computing*, 36(4): B708–B728, 2014.
- [31] J. Shen, X. Yang. Decoupled, energy stable schemes for phase-field models of two-phase incompressible flows. *SIAM Journal on Numerical Analysis*, 53(1): 279–296, 2015.
- [32] J. Shen, J. Xu, J. Yang. The scalar auxiliary variable (SAV) approach for gradient flows. *Journal of Computational Physics*, 353: 407–416, 2018.
- [33] G. Tryggvason, R. Scardovelli and S. Zaleski. *Direct Numerical Simulations of Gas-Liquid Multiphase Flows*. Cambridge University Press, New York, 2011.
- [34] S. M. Wise, C. Wang, J. S. Lowengrub. An energy-stable and convergent finite-difference scheme for the phase field crystal equation. *SIAM Journal on Numerical Analysis*, 47(3): 2269–2288, 2009.
- [35] X. Yang. Linear, first and second-order, unconditionally energy stable numerical schemes for the phase field model of homopolymer blends. *Journal of Computational Physics*, 327: 294–316, 2016.
- [36] X. Yang, L. Ju. Efficient linear schemes with unconditionally energy stability for the phase field elastic bending energy model. *Computer Methods in Applied Mechanics and Engineering*, 315: 691–712, 2017.
- [37] X. Yang, J. Zhao, Q. Wang. Numerical approximations for the molecular beam epitaxial growth model based on the invariant energy quadratization method. *Journal of Computational Physics*, 333: 104–127, 2017.